

Frictionless contact: step by step analysis and mathematical programming technique

Filippo Cucco¹, Maria Salerno², Liborio Zito³

¹*University Kore of Enna, Italy.*

E-mail: filippo.cucco@unikore.it

²*Dept. of Construction. and Mathematical Methods in Architecture, University of Naples Federico II, Italy*

E-mail: mgsalerno@tiscali.it

³*Dept. of Civil, Ambiental and Aerospace Engineering, University of Palermo, Italy.*

E-mail: lzito@diseg.unipa.it

Keywords: Multidomain SGBEM, frictionless contact, mathematical programming.

SUMMARY. The object of the paper concerns a consistent formulation of the classical Signorini's theory regarding the frictionless unilateral contact problem between two elastic bodies in the hypothesis of small displacements and strains. A variational approach employed in conjunction with the Symmetric Boundary Element Method (SBEM) leads to an algebraic formulation based on generalized quantities [1]. The contact problem is decomposed into two sub-problems: one is purely elastic, the other pertains to the unilateral contact conditions alone [2,3]. Following this methodology, the contact problem, by symmetric BEM, is characterized by symmetry and sign definiteness of the coefficient matrix, thus admitting a unique solution.

The solution of the frictionless unilateral contact problem has been obtained:

- by means of a quadratic programming problem [2], as optimization problem developed in terms of discrete variables, by using Karnak.sGbem code [4] coupled with MatLab.
- through a step by step analysis by using nodal quantities as the check elements. Indeed the detachment or contact phenomenon occurs when the traction or the displacement is greater than the cohesion or reference gap, respectively [3].

The innovative approach is given mainly by the only boundary discretization by using the SBEM approach, by the elastic relation written for each bem-e involving the only quantities of the contact zone.

In the examples some comparisons of the two strategies will be shown.

1 MIXED VARIABLE MULTIDOMAIN APPROACH

This section shows the procedure utilized to obtain, using the mixed variable multidomain approach through the symmetric Boundary Element Method (SBEM) [5], an equation connecting mechanical and kinematical weighted quantities in the contact boundaries to mechanical and kinematical nodal quantities defined in the same contact boundaries, and to the known boundary (forces and imposed displacements) and domain (body forces) actions. This expression is characterized by elastic operators containing the geometry and constitutive data.

Consider the classical Somigliana Identities (S.Is.), written for one of two contact bodies, i.e.:

$$\mathbf{u} = \int_{\Gamma} \mathbf{G}_{uu} \mathbf{f} d\Gamma + \int_{\Gamma} \mathbf{G}_{ut} (-\mathbf{u}) d\Gamma + \int_{\Omega} \mathbf{G}_{uu} \bar{\mathbf{b}} d\Omega \quad (1a)$$

$$\mathbf{t} = \int_{\Gamma} \mathbf{G}_m \mathbf{f} d\Gamma + \int_{\Gamma} \mathbf{G}_m (-\mathbf{u}) d\Gamma + \int_{\Omega} \mathbf{G}_m \bar{\mathbf{b}} d\Omega \quad (1b)$$

having domain Ω and boundary Γ .

It is subjected to plane actions, i.e. to forces $\bar{\mathbf{f}}_2$ at the portion Γ_2 of the free boundary, to displacements $\bar{\mathbf{u}}_1$ imposed at the portion Γ_1 of the constrained boundary, to body forces $\bar{\mathbf{b}}$ in Ω .

The contact between the two bodies involves the presence of the boundary Γ_0 . We want to obtain the elastic response to the external actions in terms of displacements \mathbf{u}_2 on Γ_2 and reactive forces \mathbf{f}_1 on Γ_1 , but also in terms of the displacements \mathbf{u}_0 and tractions \mathbf{t}_0 at the contact boundary Γ_0 and in terms of stresses $\boldsymbol{\sigma}$ in the domain of each body by using the mixed variable multidomain SBEM approach [5].

1.1 Governing equations of the body

Consider a generic body, here called bem-element (bem-e), characterized by the boundary Γ distinguished into three parts, free Γ_2 , constrained Γ_1 and contact Γ_0 . For this bem-e the following Dirichlet and Neumann conditions can be written:

$$\begin{aligned} \mathbf{u}_1 &= \bar{\mathbf{u}}_1 \quad \text{on } \Gamma_1 \\ \mathbf{t}_2 &= \bar{\mathbf{f}}_2 \quad \text{on } \Gamma_2 \end{aligned} \quad (2a,b)$$

If we introduce in Eqs.(2a,b) the S.Is. of the displacements and tractions, the following boundary integral equations can be obtained:

$$\begin{aligned} \mathbf{u}_1[\mathbf{f}_1, -\mathbf{u}_2, \mathbf{f}_0, -\mathbf{u}_0] + \mathbf{u}_1[\bar{\mathbf{f}}_2, -\bar{\mathbf{u}}_1^{PV}, \bar{\mathbf{b}}] + \frac{1}{2} \bar{\mathbf{u}}_1 &= \bar{\mathbf{u}}_1 \\ \mathbf{t}_2[\mathbf{f}_1, -\mathbf{u}_2, \mathbf{f}_0, -\mathbf{u}_0] + \mathbf{t}_2[\bar{\mathbf{f}}_2^{PV}, -\bar{\mathbf{u}}_1, \bar{\mathbf{b}}] + \frac{1}{2} \bar{\mathbf{f}}_2 &= \bar{\mathbf{f}}_2 \end{aligned} \quad (3a,b)$$

where a symbolic form has been used and where the typologies of the boundary are characterized by the indices introduced in the displacement and traction vectors.

It is necessary to define the unknowns \mathbf{u}_0 and \mathbf{t}_0 , related to the contact boundary Γ_0

$$\begin{aligned} \mathbf{u}_0 &= \mathbf{u}_0[\mathbf{f}_1, -\mathbf{u}_2, \mathbf{f}_0, -\mathbf{u}_0^{PV}] + \frac{1}{2} \mathbf{u}_0 + \mathbf{u}_0[\bar{\mathbf{f}}_2, -\bar{\mathbf{u}}_1, \bar{\mathbf{b}}] \\ \mathbf{t}_0 &= \mathbf{t}_0[\mathbf{f}_1, -\mathbf{u}_2, \mathbf{f}_0^{PV}, -\mathbf{u}_0] + \frac{1}{2} \mathbf{t}_0 + \mathbf{t}_0[\bar{\mathbf{f}}_2, -\bar{\mathbf{u}}_1, \bar{\mathbf{b}}] \end{aligned} \quad (4a,b)$$

where the terms $\mathbf{u}[-\mathbf{u}_0^{PV}]$ and $\mathbf{t}[\mathbf{t}_0^{PV}]$ include the presence of integrals as the Cauchy Principal Values, while the terms where $\frac{1}{2}$ occurs are the corresponding free terms.

Eqs.(3a,b) have to be rewritten in a different way

$$\begin{aligned}
\mathbf{u}_1[\mathbf{f}_1, -\mathbf{u}_2, \mathbf{f}_0, -\mathbf{u}_0] + \underbrace{\mathbf{u}_1[\bar{\mathbf{f}}_2, -\bar{\mathbf{u}}_1^{PV}, \bar{\mathbf{b}}]}_{\hat{\mathbf{u}}_1} - \frac{1}{2} \bar{\mathbf{u}}_1 &= \mathbf{0} \\
\mathbf{t}_2[\mathbf{f}_1, -\mathbf{u}_2, \mathbf{f}_0, -\mathbf{u}_0] + \underbrace{\mathbf{t}_2[\bar{\mathbf{f}}_2^{PV}, -\bar{\mathbf{u}}_1, \bar{\mathbf{b}}]}_{\hat{\mathbf{t}}_2} - \frac{1}{2} \bar{\mathbf{f}}_2 &= \mathbf{0}
\end{aligned} \tag{5a,b}$$

whereas Eqs.(4a,b) remain unchanged.

We introduce the boundary discretization into the boundary elements by performing the following modelling of all the known and unknown quantities:

$$\mathbf{f}_1 = \Psi_f \mathbf{F}_1, \quad \bar{\mathbf{f}}_2 = \Psi_f \bar{\mathbf{F}}_2, \quad \mathbf{t}_0 = \Psi_t \mathbf{F}_0, \quad \mathbf{u}_2 = \Psi_u \mathbf{U}_2, \quad \bar{\mathbf{u}}_1 = \Psi_u \bar{\mathbf{U}}_1, \quad \mathbf{u}_0 = \Psi_u \mathbf{U}_0 \tag{6a-f}$$

where Ψ_f and Ψ_u are appropriate matrices of shape functions regarding the boundary quantities. Further, the capital letters indicate the nodal vectors of the forces (\mathbf{F}_1 , $\bar{\mathbf{F}}_2$ and \mathbf{F}_0) and of the displacements ($\bar{\mathbf{U}}_1$, \mathbf{U}_2 and \mathbf{U}_0) defined at the boundary nodes.

We now perform the weighting of all the coefficients of Eqs.(4) and (5). For this purpose, the same shape functions as those modelling the causes are employed, but introduced in an energetically dual way according to the Galerkin approach [2], thus obtaining the following generalized equations:

$$\int_{\Gamma_1} \Psi_f^T (\mathbf{u}_1 - \bar{\mathbf{u}}_1) = \mathbf{0}, \quad \int_{\Gamma_2} \Psi_u^T (\mathbf{t}_2 - \bar{\mathbf{f}}_2) = \mathbf{0}, \quad \mathbf{W}_0 = \int_{\Gamma_0} \Psi_f^T \mathbf{u}_0, \quad \mathbf{P}_0 = \int_{\Gamma_0} \Psi_u^T \mathbf{t}_0 \tag{7a-d}$$

As a consequence, these latter are rewritten in the following symbolic form:

$$\begin{aligned}
\mathbf{W}_1[\mathbf{F}_1, -\mathbf{U}_2, \mathbf{F}_0, -\mathbf{U}_0] + \hat{\mathbf{W}}_1 &= \mathbf{0} \\
\mathbf{P}_2[\mathbf{F}_1, -\mathbf{U}_2, \mathbf{F}_0, -\mathbf{U}_0] + \hat{\mathbf{P}}_2 &= \mathbf{0} \\
\mathbf{W}_0 &= \mathbf{W}_0[\mathbf{F}_1, -\mathbf{U}_2, \mathbf{F}_0, -\mathbf{U}_0] + \hat{\mathbf{W}}_0 \\
\mathbf{P}_0 &= \mathbf{P}_0[\mathbf{F}_1, -\mathbf{U}_2, \mathbf{F}_0, -\mathbf{U}_0] + \hat{\mathbf{P}}_0
\end{aligned} \tag{8a-d}$$

or in the following equivalent block system:

$$\begin{array}{c|cc|cc|c|c}
\mathbf{0} & \mathbf{A}_{u1,u1} & \mathbf{A}_{u1,f2} & \mathbf{A}_{u1,u0} & \mathbf{A}_{u1,f0} & \mathbf{F}_1 & \hat{\mathbf{W}}_1 \\
\mathbf{0} & \mathbf{A}_{f2,u1} & \mathbf{A}_{f2,f2} & \mathbf{A}_{f2,u0} & \mathbf{A}_{f2,f0} & -\mathbf{U}_2 & \hat{\mathbf{P}}_2 \\
\mathbf{W}_0 & \mathbf{A}_{u0,u1} & \mathbf{A}_{u0,f2} & \mathbf{A}_{u0,u0} & \bar{\mathbf{A}}_{u0,f0} & \mathbf{F}_0 & \hat{\mathbf{W}}_0 \\
\mathbf{P}_0 & \mathbf{A}_{f0,u1} & \mathbf{A}_{f0,f2} & \bar{\mathbf{A}}_{f0,u0} & \mathbf{A}_{f0,f0} & -\mathbf{U}_0 & \hat{\mathbf{P}}_0
\end{array} = \tag{9}$$

In the latter block equation the matrix \mathbf{A} is symmetric. Moreover, the submatrices and the subvectors $\hat{\mathbf{W}}, \hat{\mathbf{P}}$ are formed by coefficients obtained through a double integration according to the SBEM strategy. In detail, the first and second rows represent the Dirichlet and Neumann conditions written in weighted form $\mathbf{W}_1 - \hat{\mathbf{W}}_1 = \mathbf{0}$ and $\mathbf{P}_2 - \hat{\mathbf{P}}_2 = \mathbf{0}$. The remaining rows regard the

weighting of the displacements and tractions in the contact zones. The terms $\bar{\mathbf{A}}_{u0,f0} = \bar{\mathbf{A}}_{f0,u0}$ are symmetric and include the weighting of the CPV integrals and of the corresponding free terms.

In Eq.(9) some coefficients show singular or hyper-singular kernels. These difficulties were overcome within the SBEM approach by using different techniques. The reader can refer to Panzeca et al. [1, 5] for a more detailed discussion of the computational aspects and for the related references.

Eq.(9) can be expressed in compact form in the following way:

$$\begin{aligned}\mathbf{0} &= \mathbf{A} \mathbf{X} + \mathbf{A}_0 \mathbf{X}_0 + \hat{\mathbf{L}} \\ \mathbf{Z}_0 &= \mathbf{A}_0^T \mathbf{X} + \mathbf{A}_{00} \mathbf{X}_0 + \hat{\mathbf{L}}_0\end{aligned}\quad (10a,b)$$

where the following positions were set

$$\mathbf{Z}_0 = \begin{Bmatrix} \mathbf{W}_0 \\ \mathbf{P}_0 \end{Bmatrix}, \quad \mathbf{X} = \begin{Bmatrix} \mathbf{F}_1 \\ -\mathbf{U}_2 \end{Bmatrix}, \quad \mathbf{X}_0 = \begin{Bmatrix} \mathbf{F}_0 \\ -\mathbf{U}_0 \end{Bmatrix}, \quad \hat{\mathbf{L}} = \begin{Bmatrix} \hat{\mathbf{W}}_1 \\ \hat{\mathbf{P}}_2 \end{Bmatrix}, \quad \hat{\mathbf{L}}_0 = \begin{Bmatrix} \hat{\mathbf{W}}_0 \\ \hat{\mathbf{P}}_0 \end{Bmatrix} \quad (11a-e)$$

The vector \mathbf{Z}_0 collects the generalized (or weighted) displacement \mathbf{W}_0 and traction \mathbf{P}_0 subvectors defined at the boundaries in contact, obtained as the response to all the known and unknown actions, regarding the boundary and domain quantities. By performing variable condensation through the replacement of the vector \mathbf{X} extracted from Eq.(10a) into Eq.(10b), one obtains:

$$\mathbf{Z}_0 = \mathbf{D}_{00} \mathbf{X}_0 + \hat{\mathbf{Z}}_0 \quad (12)$$

where one sets

$$\mathbf{D}_{00} = \mathbf{A}_0^T \mathbf{A}^{-1} \mathbf{A}_0 - \mathbf{A}_{00}, \quad \hat{\mathbf{Z}}_0 = -\mathbf{A}_0^T \mathbf{A}^{-1} \hat{\mathbf{L}} + \hat{\mathbf{L}}_0, \quad (13a,b)$$

Eq.(12) is a characteristic equation written for each bem-e. It relates the generalized (or weighted) displacements and tractions, collected in \mathbf{Z}_0 , defined at the contact zone Γ_0 , to the force and displacement nodal quantities \mathbf{X}_0 and to the load vector $\hat{\mathbf{Z}}_0$. Moreover \mathbf{D}_{00} is an appropriate stiffness-flexibility matrix of the bem-e being examined.

1.2 Bem-element assembly

This strategy is based on the approach of multi-connected bodies handled by using the symmetric BEM, recently introduced [1,5,6].

Let us start by considering the two bodies in contact and for each of these Eq.(12). Thus we obtain two global relations related to the bem-elements considered, i.e.:

$$\begin{Bmatrix} \mathbf{Z}_0^A \\ \mathbf{Z}_0^B \end{Bmatrix} = \begin{Bmatrix} \mathbf{D}_{00}^A & \mathbf{0} \\ \mathbf{0} & \mathbf{D}_{00}^B \end{Bmatrix} \begin{Bmatrix} \mathbf{X}_0^A \\ \mathbf{X}_0^B \end{Bmatrix} + \begin{Bmatrix} \hat{\mathbf{Z}}_0^A \\ \hat{\mathbf{Z}}_0^B \end{Bmatrix} \quad (14)$$

or in compact form

$$\mathbf{Z}_0 = \mathbf{D}_{00} \mathbf{X}_0 + \hat{\mathbf{Z}}_0 \quad (15)$$

formally equal to Eq.(12).

We introduce the nodal vector \mathbf{Y}_0 of the mechanical and kinematical unknowns related to the assembled system regarding the Γ_0 boundary and perform a suitable nodal variable condensation through the matrices of equilibrium \mathbf{L}^T and of compatibility \mathbf{N} , respectively:

$$\begin{array}{c} \left| \begin{array}{c} \mathbf{F}_0^A \\ -\mathbf{U}_0^A \\ \mathbf{F}_0^B \\ -\mathbf{U}_0^B \end{array} \right| = \left| \begin{array}{cc} (\mathbf{L}^A)^T & \mathbf{0} \\ \mathbf{0} & \mathbf{N}^A \\ (\mathbf{L}^B)^T & \mathbf{0} \\ \mathbf{0} & \mathbf{N}^B \end{array} \right| \left| \begin{array}{c} \mathbf{F}_0 \\ -\mathbf{U}_0 \end{array} \right| \quad i.e. \quad \mathbf{X}_0 = \mathbf{E} \mathbf{Y}_0 \end{array} \quad (16)$$

The latter relation has to be considered as a strong regularity condition related to the nodal quantities.

The same transposed matrices \mathbf{L} and \mathbf{N}^T define the weighted equilibrium and compatibility, respectively.

$$\left| \begin{array}{cc|cc} \mathbf{L}^A & \mathbf{0} & \mathbf{L}^B & \mathbf{0} \\ \mathbf{0} & (\mathbf{N}^A)^T & \mathbf{0} & (\mathbf{N}^B)^T \end{array} \right| \left| \begin{array}{c} \mathbf{W}_0^A \\ \mathbf{P}_0^A \\ \mathbf{W}_0^B \\ \mathbf{P}_0^B \end{array} \right| = \left| \begin{array}{c} \mathbf{0} \\ \mathbf{0} \end{array} \right| \quad i.e. \quad \mathbf{E}^T \mathbf{Z}_0 = \mathbf{0} \quad (17)$$

The latter relation has to be considered as a weak regularity condition related to the weighted quantities.

Eqs.(16,17) utilized with Eqs.(15) give rise to the following relation:

$$\mathbf{K}_{00} \mathbf{Y}_0 + \hat{\mathbf{f}}_0 = \mathbf{0} \quad (18)$$

where

$$\mathbf{K}_{00} = \mathbf{E}^T \mathbf{D}_{00} \mathbf{E}, \quad \hat{\mathbf{f}}_0 = \mathbf{E}^T \hat{\mathbf{Z}}_0 \quad (19)$$

Eq.(18) can be rewritten in the following form

$$\left| \begin{array}{cc|c} \mathbf{K}_{W_0W_0} & \mathbf{K}_{W_0P_0} & \mathbf{F}_0 \\ \mathbf{K}_{P_0W_0} & \mathbf{K}_{P_0P_0} & -\mathbf{U}_0 \end{array} \right| + \left| \begin{array}{c} \hat{\mathbf{L}}_{W_0} \\ \hat{\mathbf{L}}_{P_0} \end{array} \right| = \left| \begin{array}{c} \mathbf{0} \\ \mathbf{0} \end{array} \right| \quad (20)$$

By performing a diagonalization process of Eqs. (20), one obtains

$$\left| \begin{array}{c|c} \mathbf{K}_{W_0W_0} & \mathbf{0} \\ \hline \mathbf{0} & \tilde{\mathbf{K}}_{P_0P_0} \end{array} \right| \left| \begin{array}{c} \mathbf{F}_0 \\ -\mathbf{U}_0 \end{array} \right| + \left| \begin{array}{c} \tilde{\mathbf{L}}_{W_0} \\ \tilde{\mathbf{L}}_{P_0} \end{array} \right| = \left| \begin{array}{c} \mathbf{0} \\ \mathbf{0} \end{array} \right| \quad (21)$$

where

$$\begin{aligned} \tilde{\mathbf{K}}_{P_0P_0} &= \mathbf{K}_{P_0P_0} - \mathbf{K}_{W_0P_0}^T \mathbf{K}_{W_0W_0}^{-1} \mathbf{K}_{W_0P_0}, \\ \tilde{\mathbf{L}}_{P_0} &= \hat{\mathbf{L}}_{P_0} - \mathbf{K}_{W_0P_0}^T \mathbf{K}_{W_0W_0}^{-1} \hat{\mathbf{L}}_{W_0}, \\ \tilde{\mathbf{L}}_{W_0} &= \hat{\mathbf{L}}_{W_0} - \mathbf{K}_{W_0P_0} \tilde{\mathbf{K}}_{P_0P_0}^{-1} \tilde{\mathbf{L}}_{P_0} \end{aligned} \quad (22)$$

The two equations extracted from Eq.(21) $\mathbf{K}_{W_0W_0} \mathbf{F}_0 + \tilde{\mathbf{L}}_{W_0} = \mathbf{0}$ and $\tilde{\mathbf{K}}_{P_0P_0} (-\mathbf{U}_0) + \tilde{\mathbf{L}}_{P_0} = \mathbf{0}$ represent the force and the displacement methods, respectively, based on the mixed boundary values in terms of the symmetric BEM. These equations can be used to obtain the solution in a contact-detachment process as a linear complementary problem, through a step-by-step procedure, or to solve a minimum problem of the total potential energy through a quadratic programming.

2 CONTACT-DETACHMENT PROBLEM

The analysis process concerns two bodies in contact, A and B, which are subjected to external actions, constant or variable in time. In both hypotheses, the problem appears nonlinear because the external actions modify the zones that characterize the boundary of the two bodies: in particular the typifying of the boundaries Γ_2 and Γ_0 changes partially.

Let us consider the boundary conditions of the Signorini unilateral contact problem rewritten in nodal form, as discussed in a more extensive form by Panzeca et al. in [3]:

$$\begin{aligned} \tilde{\mathbf{n}}^A (\mathbf{W}_2^A - \mathbf{W}_2^B) &\leq \mathbf{H}, \quad \mathbf{C} = \mathbf{0} && \text{gap condition} \\ \tilde{\mathbf{n}}^A \mathbf{P}_0^A &\leq \mathbf{C}, \quad \mathbf{H} = \mathbf{0} && \text{contact condition} \\ [\tilde{\mathbf{n}}^A (\mathbf{W}_2^A - \mathbf{W}_2^B) - \mathbf{H}] [\tilde{\mathbf{n}}^A \mathbf{P}_0^A - \mathbf{C}] &= 0 && \text{complementarity condition} \end{aligned} \quad (23a-c)$$

where the vector \mathbf{n}^A is the external unit vector at the discretized boundary elements of the body A and where the following positions are valid:

$$\mathbf{H} = \int_{\Gamma_2} \tilde{\psi}_f h, \quad \mathbf{C} = \int_{\Gamma_0} \tilde{\psi}_u c \quad (24a,b)$$

The vector \mathbf{H} represents the weighted distance between two boundary elements of Γ_2^A and Γ_2^B , computed along the normal vector \mathbf{n}^A , in the zone of potential contact, whereas the vector \mathbf{C} indicates the weighted cohesion between the boundary elements which are in contact, in the zone of potential detachment.

In this paper, only the detachment approach is considered.

The solution of the frictionless detachment problem can be obtained as a solution of a linear complementarity problem through a recursive step-by-step analysis verifying at every step when the inequality (23b) is verified. As a consequence, a change in the typifying of the boundaries Γ_2 and Γ_0 of the bodies in contact, occurs.

The same solution can be obtained directly as a quadratic programming problem through the introduction of the total potential energy in terms of discrete variables associated with the boundary nodes involved in the detachment phenomenon. For this purpose, let us consider the functional $\Pi[\mathbf{F}_0]$, similarly to what is shown by Polizzotto [2], where the variables on the interface boundary are considered as the average of the nodal quantities, evaluated in the direction defined by the normal vector \mathbf{n}^A , i.e.:

$$\Pi[\mathbf{F}_0] = \frac{1}{2} \mathbf{F}_0^T \mathbf{K}_{w_0 w_0} \mathbf{F}_0 + \mathbf{F}_0^T \tilde{\mathbf{L}}_{w_0} \quad (25)$$

obtained by using the first of Eqs.(21),

According to this strategy the solution of the detachment problem is obtained as the minimum of the functional (25) in the following way:

$$\min_{(\mathbf{F}_0)} \Pi[\mathbf{F}_0], \quad \text{s.t.} \quad \mathbf{F}_0 \leq \mathbf{C} \quad (26)$$

The condition $\mathbf{F}_0 = \mathbf{C}$ has to be considered as limit condition for the detachment phenomenon.

3 NUMERICAL RESULTS

In order to show the efficiency of the proposed method, two structures have been considered and subjected to external actions, constant in time. In both the cases, the detachment phenomenon is treated in absence of friction and sliding. Indeed, the package of the Karnak.sGbem program regarding the friction and sliding is yet not active.

3.1 First example

In Figure 1a the beam is subjected to a load $q = 1000 \text{ daN/m}$. The material characteristics are Young's modulus $E = 50000 \text{ daN/cm}^2$, Poisson's ratio $\nu = 0.22$ and $c = 0$. Moreover, the beam is subdivided into two substructures whose the contact zone, discretized into 104 boundary elements each being cm 0.38 long, was analyzed. In Figure 1b a diagram is given which shows the nodal forces of the contact nodes, provided by step-by-step analysis using the SBEM strategy, as a function of the contact boundary. The resulting detachment zone by step-by-step analysis is cm. 33,85 long, whereas by the quadratic programming via Matlab is cm. 33,08 long.

It is opportune to remember that the detachment is found by using a step-by-step analysis through the normal weighted forces and by using a quadratic programming through the average of the nodal forces, evaluated in the normal direction.

In the step-by-step analysis with the Karnak.sGbem program [4], the tangential tractions are present, whereas in the functional Π these quantities are not considered. Nevertheless, the two approaches give rise to similar results because of the symmetry of the beam.

In Figure 1c a detail of the detachment zone, obtained through a step-by-step analysis, is shown.

When the beam becomes squat, we noted a difference in the results of the detachment zone.

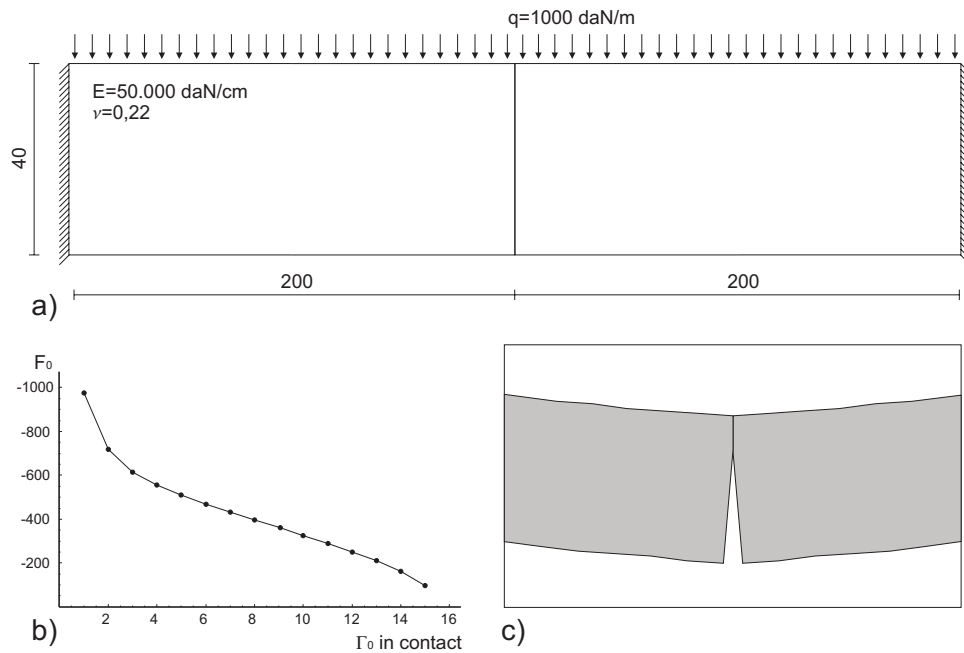


Figure 1: a) Beam built-in at the extremities, b) diagram of the contact forces in function of the contact boundary, c) detachment zone in the step-by-step analysis.

3.2 Second example

A concrete block shown in Figure 2a, having as physical characteristics $E = 300000 \text{ daN/cm}^2$, $\nu=0.25$ and $c=0$ is constrained to the ground. Four iron rods ($2\phi 12 + 2\phi 12$) connect an iron structural system plate+H bar to the concrete block. The physical characteristics of the steel elements are $E = 2200000 \text{ daN/cm}^2$ and $\nu=0.3$, whereas the geometrical characteristics of the H-bar are $I = 5696 \text{ cm}^4$, $A = 78.1 \text{ cm}^2$. In this plane problem the iron rods have been substituted by two steel bars, each having rectangular section $A = 1 \bullet 2.26 \text{ cm}^2$. At the H-bar top a vertical load $N = 100000 \text{ daN}$ has been applied, distant $e = 10 \text{ cm}$ from the barycentre axis. As a consequence, since a stress distribution mechanically equivalent to the vertical load must be applied at the H-bar top, the following stress values $\sigma_c = -3036.03 \text{ daN/cm}^2$ and $\sigma_t = +475.21 \text{ daN/cm}^2$ must be considered at the extremes of the section. The cohesion between the plate and the concrete is obviously absent.

The employed approach involves preliminarily the macro-zoning of the structural system into 7 sub-structures, each of their discretized into the boundary elements (bem-e):

- two flanges of the steel section: 32 bem-e for each sub-structures,
- the stem of the H-bar: 34 bem-e,
- two iron rods 16 bem-e for each sub-structures,
- the plate 72 bem-e,
- the concrete block 152 bem-e.

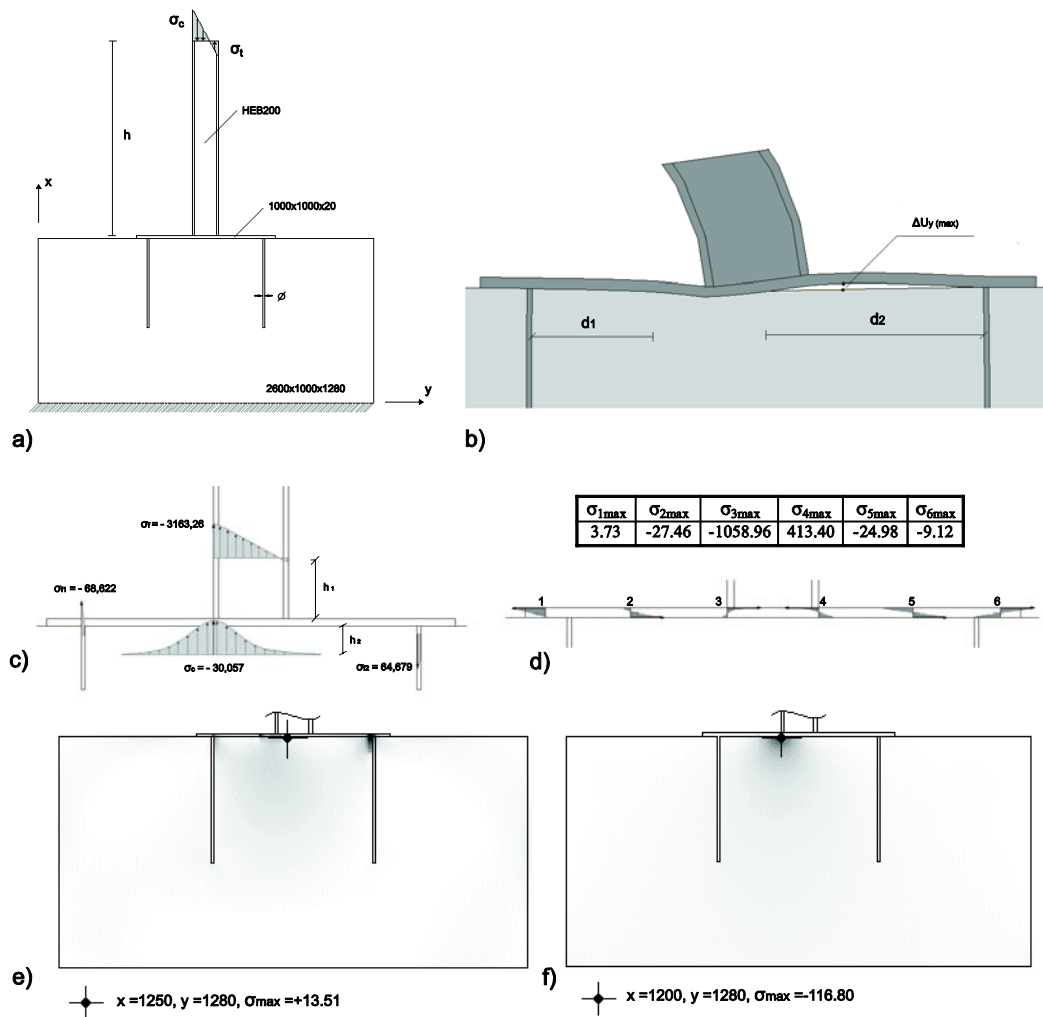


Figure 2: a) An iron structural system plate+H bar connected to concrete block, b) The strained shape, c) The normal stress distributions in the concrete block and H bar and d) in the plate, e), f) The principal traction and compression stress mappings.

Because of the couple action, a detachment between the plate and the below concrete block happens through a step by step procedure, whose effects are shown in Figure 2b. This procedure contemplates the comparison between the weighted tractions with the value of the weighted cohesion (null in this example) at every beam-e, using the eq.(23b). The detachment phenomenon involves two boundary detachments having the following dimensions $d_1 = 26$ cm (13 beam-e) and $d_2 = 46$ cm (23 beam-e).

In Figure 2b the strained shape is shown by considering an amplified scale and by having the H-bar cut off, whereas in Figure 2c the stress diagrams are valued at the H-bar ($h_1 = 18$ cm) and near to concrete compressed zone ($h_2 = 10$ cm). Their evaluations are made through the Somigliana

Identities by employing only the boundary and domain quantities of the examining sub-structure. It is possible to note that the stress distribution in the H-bar is different from that acting at the top; this difference depends on the plate rotation, caused by the detachment. In fact, because of constrained extreme rotation and of the H-bar flexional deformation, the horizontal relative displacement between the free extreme and the displacement of the section distant h_1 from the constraint is $e_1 = 0.935 - 0.034 = 0.901$ cm. Therefore the new eccentricity of the load N follows $e = 10 + e_1 = 10.901$ cm and, as a consequence, the linear stress distribution takes on the maximum compression and traction analytical values: $\sigma_c = -3194.20$ daN/cm² and $\sigma_t = +634.01$ daN/cm². The compression value is almost similar to the value that is obtained by using the Karnak.sGbem program [4]: indeed, it comes out $\sigma_c = -3163.26$ daN/cm², with 1% of percentage error.

In Figure 2d the normal stress diagrams are shown in several sections, all having a linear shape. The maximum values of each distribution are included in a table of the same drawing.

The Figures 2e,f show the principal traction and compression stress mappings of the concrete block with the indication of the maximum values.

References

- [1] Panzeca T., Cucco F., Terravecchia S., "Symmetric boundary element method versus Finite element method". *Comp. Meth. Appl. Mech. Engng.* **191**, 3347-3367 (2002).
- [2] Polizzotto C., "Variational boundary-integral-equation approach to unilateral contact problems in elasticity". *Computational Mechanics.* **13**, 100-115 (1993).
- [3] Panzeca T., Salerno M., Terravecchia S., Zito., "The symmetric Boundary Element Method for unilateral contact problems". *Comp. Meth. Appl. Mech. Engng.* **197**, 2667-2679 (2008).
- [4] Cucco F., Panzeca T., Terravecchia S., "The program Karnak.sGbem Release 2.1", Palermo University. (2002).
- [5] Panzeca T., Salerno M., "Macro-elements in the mixed boundary value problems", *Comp. Mech.* **26**, 437-446 (2000).
- [6] Perez-Gavilan J.J. and Aliabadi M.H., "Symmetric Galerkin BEM for Multi-connected bodies", *Commun. Numer. Meth. Engng.* **17**, 761-770 (2001).